Research Article

Space Science Journal

High-Resolving Conical Electrostatic Energy Analyzer for Plasma Flows Investigations

A.M. Ilyin*, N.R. Guseinov and M.A. Tulegenova

National Nano lab, Almaty, 050040, Kazakhstan

*Corresponding Author
A.M. Ilyin, National Nano lab, Almaty, 050040, Kazakhstan.

Submitted: 2024, Jan 01; **Accepted**: 2024, Jan 29; **Published**: 2024, Jan 29

Citation: Ilyin, A. M., Guseinov, N. R., Tulegenova, M. A. (2024). High-Resolving Conical Electrostatic Energy Analyzer for Plasma Flows Investigations. *Space Sci J, 1*(1), 1-7.

Abstract

The paper presents numerically calculated model of the new electrostatic energy analyzer based on a bounded conical field, separating and focusing a flow of charged particles, having velocity parallel or nearly parallel to the axis of symmetry of the analyzer. The calculations show second order focusing with very large acceptance aperture, what is important for obtaining accurate data of intensity, energy characteristics, main direction of space particle flows, which are characterized by very low density. These data are important for monitoring and forecasting abnormal electromagnetic events over the Earth and near-Earth space which can effect on normal operation and even on the safety of the crew of space station. A combination of high energy resolution with large aperture, simple compact design and control and remote fine tuning makes the instrument very promising for space technologies.

1. Introduction

Electron spectroscopy techniques, that originated many years ago, are currently being developed and applied for solving many scientific and technological problems. Judging by the number of recent publications these methods have shown very effective use in different areas: materials science [1-15]. Nuclear engineering [16-19]. Nanotechnologies and biology [20-39]. In the space plasma explorations [40-50]. Next we consider some applications of the electron spectroscopy devices for exploration of directed near- Earth space charged particle streams. In quarter - spherical electron energy analyzers were designed for study in-space electron distribution in energy range from 1 up to 3 keV and in a 120 x 360 degrees solid angle sector [41]. The energy interval used covers the thermal solar wind plasma electrons. Instrumental calibrations shown the main characteristics in a good agreement with theoretical calculations. In the papers [40,42]. A plasma package was aimed for study the solar wind- Mars and Venus interaction. A well-known top-hat electrostatic energy analyzer in a compact design was used in the paper [45]. For measurements within the space near Mars in energy range 0.01 - 20 keV. In the interesting work [48]. The top-hat design in general was used as a model for expected response of the instrument in simulated plasma conditions. Have also been real parameters of fast solar wind streams and coronal mass ejections used for investigations the characteristics of the example instrument and the accuracy of the analysis. In paper some important moments relate to interactions between space plasma - spacecraft materials are presented [51]. Energetic particles from space plasma flow can destroy the structure of the material and change chemical system of surface of the spacecraft. For example, monitoring of space charged particle flows (like solar wind) is very important for forecasting possible abnormal electromagnetic effects over the Earth and near-Earth space. Such effects may cause failures in connection systems, air- and spacecraft operations, in electronic systems, undesirable effects due the interaction of space particle stream with spacecraft material, for example, its surface charging. Moreover, they are dangerous for the orbital spacecraft crew due to the action of fast charged particle flow and electromagnetic radiation [51-54]. During these events crew on the orbital station (ISS) need to seek screen or shelter and to stop spacewalks. Therefore, scientists need fine instruments for monitoring and predicting of such events. There are many well-known different types of electrostatic energy analyzers, which have been developed for solving various scientific and technological problems. Judging to number of publications, the most energy analyzers for space explorations are based on the different modifications of "top-hat" systems [41-49]. Hemispherical [55-64] and retarding field analyzers [64-72]. Cusp-type analyzer [73,74]. Practically all of the mentioned analyzers are of large size, use complex configuration electrodes with large spaces of fringing fields and sets of electrodes for mitigation of their affect [57-63]. which make the design and electrical power spacecraft's system more complex. Therefore, there was a necessity in creation of

electrostatic energy analyzers, with high characteristics, combined with simple enough electrode configuration and a compact design. For example, in [75-77]. Designs, making measurements of space plasma faster are presented. Instruments, based on the bounded cylindrical face-field involving lots of modifications [3,16-21,78-84]. have been developed. Return to the old idea of using low-conical mirror in CMA case [85]. instead of cylindrical ones essentially increases possibilities for using conical energy analyzers and more complex analyzing systems, involving lots of modifications [22,86-88]. Such analyzers can effectively function in very different applications, for study remote objects, point - and large-size objects. For example, presented instrument can measure the energetic and intensity fine-characteristics of as an Earth-lab plasma charged particle beam, as well a space charged particle flow with detecting the exact direction of moving. Moreover, it can be used for detecting the flow of secondary electrons, which give information about composition and state of the spacecraft's surface, interacting with space plasma streams.

2. Calculations

In this paper we consider some focusing properties of a conical face-field analyzer, schematically presented in the Fig.1, aimed for plasma flows research.

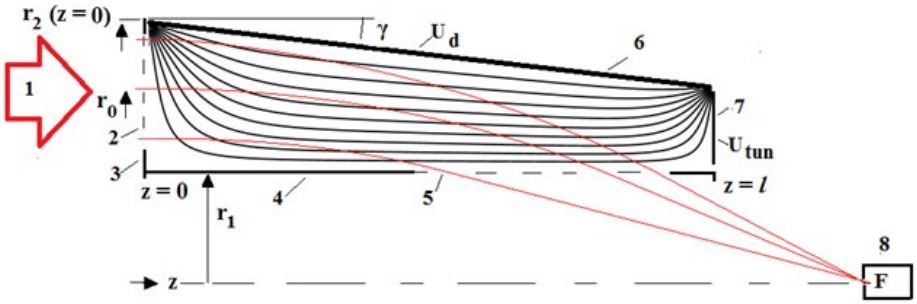

Figure 1: The schematic cross-section view (the upper part) of the analyzer presented with equipotential lines of the electrostatic focusing field. 1- charged particle beam; 2 - the annular entrance window, made in the front boundary electrode 3; 4 - the inner cylindrical electrode (usually grounded) with the exit slit 5; 6- the main focusing conical electrode at which the deflection potential Ud is applied; 7 –the rear boundary electrode to which a small tuning potential Utun is applied; 8 – the detector with a small diaphragm, and focus F at the axis of symmetry.

As one can see from Fig.1 the focusing field is restricted by the coaxial inner cylinder and truncated-cone outer electrode with two boundaries, which are perpendicular to the axis of symmetry. Mathematically, the generated field is a solution of the Laplace Eq.: $\Delta U(r,z)=0$ with the boundary conditions $U(r_1,z)=U(r,0)=0; U(r,l)=U_{tun}, U(r_2(z),z)=U_d$

where

$$r_2(z)=r_2(0)-\gamma\cdot z \qquad (1)$$

In (1) γ is the conicity factor, which can have different signs depending on the direction of the cone. The use of the (1) is justified by known small angle approximation: tg (γ) ~ γ which is true up to values of about 0.21 radian (~ 10-14 deg). Hereinafter r1 is taken as a unit of length.

$$U(r,z)=\frac{4\cdot U_d}{\pi}\cdot\sum_{m=0}^{\infty}\frac{\sin\left((2m+1)\frac{\pi\cdot z}{l}\right)}{2m+1}\cdot\frac{F_m(r)}{F_m(r_2(z)}+$$

$$\frac{4\cdot U_{tun}}{\pi}\cdot\sum_{m=0}^{\infty}\frac{\sin\left((2m+1)\frac{\pi\cdot(r-1)}{r_2(z)-1}\right)}{2m+1}\cdot\frac{I_1(2m+1)\cdot\pi\cdot z/r_2(z)}{I_1(2m+1)\cdot\pi\cdot l/r_2(z)}$$

$$F_m(r_2(z))=I_0(k_m r_2(z))\,K_0(r_2(z))-I_0(r_2(z))\,K_0(k_m r_2(z)) \qquad (2)$$

$$k_m=(2m+1)\frac{\pi}{l}$$

I_0 , K_0 and I_1 are well known modified Bessel functions .

An investigation of focusing properties was performed by numerical calculations of trajectories and determining the crossing points at the axis of symmetry. The system of non- relativistic classical equations for charged particle motion in the field (2) is given by (3), where q = e / m is the specific charge of the particle.

$$\ddot{z} = -q \cdot \partial U(r,z)/\partial z$$
$$\ddot{r} = -q \cdot \partial U(r,z)/\partial r \qquad (3)$$

Calculations were performed by using the Runge - Kutta 4th order method with absolute accuracy of the final coordinate about 0.0003. The technical details of the numerical computer calculations were mostly as in our published papers [22,3,78]. Principal data on the analyzer are given in the Table. The second order focusing regime has been found by a corresponding choice of dimensionless energy coefficient $G = E_0 / eU_d = 8.5$ (with E_0 - the initial kinetic energy of a particle by entering to analyzer, and U_d - the deflection potential, applied to the outer conical electrode). A higher value of G is very suitable for measurements of in-space charged particles flows with larger energies E_0 because it can be controlled by a lower focusing potential U_d. It should be noted, that in the case unforeseen external influences (like solar wind or magnetic disturbances) affect focusing during the space mission, using the tuning potential will restore the required mode of focusing and operation.

Some examples of the calculated tuning effect are illustrated in the Table by ΔF - the shift of F along axis due to small variation of U_{tun}.

Principal parameters of the analyzer								
l	**γ**	**r2(z =0)**	**AW**	**F**	**Utun / ΔF**	**G**	**D_E**	**R_E**
5.7	**0.12 / 6.5°**	**2.4**	**~ 0.9r_1**	**7.18**	**0.05U_d / - 0.021r_1** **-0.05 U_d / 0.018r_1**	**8.5**	**6.1**	**0.2%**

Table

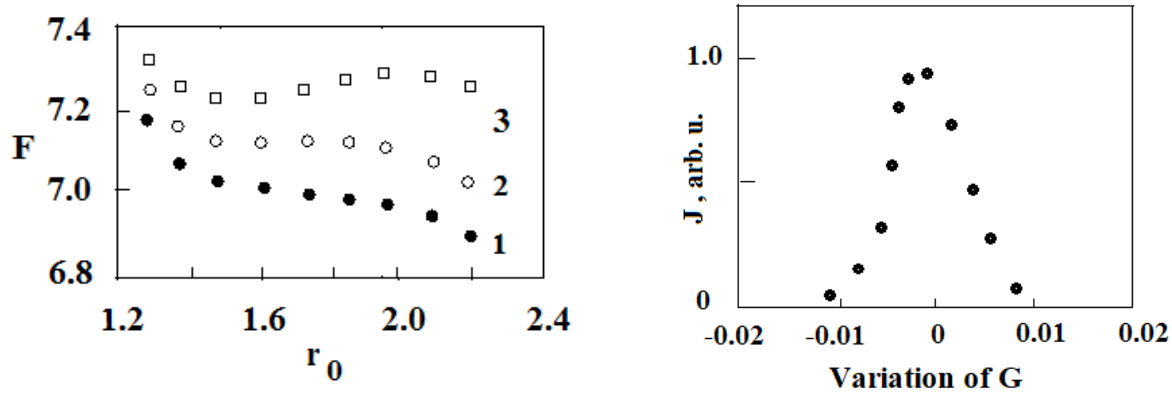

a b

Figure 2 a) Typical behavior of the aberration figures calculated for the analyzer. Aberration graphs were calculated for a following set of principal geometric parameters: *l* = 5.7 r_2 (z=0) = 2.4, coordinate of the central trajectory r0 = 1.75; γ = : 1 - 0.13; 2 – 0.12; 3 – 0.11; b) The energy transmission function J was calculated for γ = 0.12.

From aberration graphs presented in Fig.2, a one can see the essential effect of the field conicity on the focusing characteristics. Figures presented have the shape like to cubic parabola with a central inflection point, indicating the sharp second-order focusing. The small asymmetry of the transmission function is caused by the complex configuration of the focusing field, especially near the entrance window. The angular resolution averaged over the entering window is about 0.3 -0.4o. The dispersion of this analyzer was calculated by using the expression

$$D_E = (\frac{\Delta z}{\Delta E}) \cdot E \qquad (4)$$

where Δz were the finite segments obtained by trajectory for the small energy shift ΔE. According to (4) DE was estimated to be on average as large as 6.1 for γ = 0.12. For numerical calculations the energy resolution is commonly defined as $R_E = (D_E / \Delta z)^{-1}$, where Δz is a projection of the part of the aberration figure around a central part on the F axis. The energy resolution R_E calculated with the large input annular window AW (See Table), will allow obtaining data on the fine energy structure of a low-density flow.

3. Conclusion

The focusing properties of a new type of electrostatic energy analyzer, on the base of a conical face-field, were numerically calculated. Results show second-order focusing with very large aperture, when entering space charged particle beam moving nearly along to the symmetry axis. The instrument may detect and measure performances of the plasma flow surrounding spacecraft, exact direction of moving and interaction with the outer surface. Moreover, the analyzer can be remotely deployed to the surface for giving the fine energy performances of emitted secondary particles, for example, Auger electrons, giving data about spacecraft's surface elemental composition. Very simple, compact design and remote control are very important factors for such instrument to be used in-space explorations.

Authors have no conflicts of interest to disclose

References

1. Stifter, D. (2020). Surface Analytics with X-Ray Photoelectron and Auger Electron Spectroscopy on Coated Steel Sheets. Surface and Interface Science: Volume 10: Applications of Surface Science II, 10, 475-511.
2. Newman, J. G., Hammond, J. S., Davis, B. H., Suo, Z., Beech, I., Paul, D. F., & Avci, R. (2017). Auger electron spectroscopy analysis of pit initiation at MnS nano-inclusions in carbon steel. Microscopy and Microanalysis, 23(S1), 2258-2259.
3. Ilyin, A. M. (2003). New class of electrostatic energy analyzers with a cylindrical face-field. Nuclear Instruments and Methods in Physics Research Section A: Accelerators, Spectrometers, Detectors and Associated Equipment, 500(1-3), 62-67.
4. Hofmann, S., & Hofmann, S. (2013). Practice of Surface and Interface Analysis with AES and XPS. Auger-and X-Ray Photoelectron Spectroscopy in Materials Science: A User-Oriented Guide, 409-449.
5. J.H. Moor, C.C. Davis, M.A. Coplan, S.C. Greer. Building Scientific Apparatus. Cambridge University Press. 2009, 647 p.
6. Werner, W. S. (2010). Electron transport for spectrum analysis and experiment design. Journal of Electron Spectroscopy and Related Phenomena, 178, 154-177.
7. Radvanyi, E., De Vito, E., Porcher, W., Danet, J., Desbois, P., Colin, J. F., & Larbi, S. J. S. (2013). Study of lithiation mechanisms in silicon electrodes by Auger Electron Spectroscopy. Journal of Materials Chemistry A, 1(16), 4956-4965.
8. Mahoney, J., Monroe, C., Swartley, A. M., Ucak-Astarlioglu, M. G., & Zoto, C. A. (2020). Surface analysis using X-ray photoelectron spectroscopy. Spectroscopy Letters, 53(10), 726-736.
9. Debehets, J., Homm, P., Menghini, M., Chambers, S. A., Marchiori, C., Heyns, M., ... & Seo, J. W. (2018). Detecting Fermi-level shifts by Auger electron spectroscopy in Si and GaAs. Applied Surface Science, 440, 386-395.
10. Lefebvre, J., Galli, F., Bianchi, C. L., Patience, G. S., & Boffito, D. C. (2019). Experimental methods in chemical engineering: X-ray photoelectron spectroscopy-XPS. The Canadian Journal of Chemical Engineering, 97(10), 2588-2593.
11. Fischer, Ingo, and Stephen T. Pratt. "Photoelectron spectroscopy in molecular physical chemistry." Physical Chemistry Chemical Physics 24.4 (2022): 1944-1959.
12. Gorelik, V. (2012). Cylindrical mirror analyzer with entrance angles from 90.5° to 98.5°. Journal of Electron Spectroscopy and Related Phenomena, 185(3-4), 53-54.
13. Kobayashi, E., Seo, J., Nambu, A., & Mase, K. (2007). Development of a miniature double-pass cylindrical mirror electron energy analyzer (DPCMA), and its application to Auger photoelectron coincidence spectroscopy (APECS). Surface science, 601(17), 3589-3592.
14. Edwards Jr, D. (2016). The segmented cylindrical mirror analyzer (CMA). Journal of Electron Spectroscopy and Related Phenomena, 209, 46-52.
15. Edwards Jr, D. (2016). Improving the performance of the Cylindrical Mirror Analyzer II: reducing the dependence of energy resolution on sample position. Journal of Electron Spectroscopy and Related Phenomena, 212, 62-73.
16. Ilyin, A. M., & Golovanov, V. N. (1996). Auger spectroscopy study of the stress enhanced impurity segregation in a Cr□ Mo□ V steel. Journal of nuclear materials, 233, 233-235.
17. Ilyin, A. M. (1998). Some features of grain boundary segregations in sensitized austenitic stainless steel. Journal of nuclear materials, 252(1-2), 168-170.
18. Ilyin, A. M., Neustroev, V. S., Shamardin, V. K., Shestakov, V.

P., Tazhibaeva, I. L., & Krivchenkoa, V. A. (2000). Influence of combined thermomechanical treatment on impurity segregation in ferritic–martensitic and austenitic stainless steels. Journal of nuclear materials, 283, 694-696.
19. Ilyin, A. M., Tazhibaeva, I. L., & Borisov, B. A. (2002). Effect of thermal cycling on impurity grain boundary segregation in maraging steel. Journal of nuclear materials, 307, 475-478.
20. Guseinov, N. R., & Ilyin, A. M. (2021). Electrostatic energy analyzer for nanotechnology applications. Journal of Electron Spectroscopy and Related Phenomena, 246, 147031.
21. Ilyin, A. M. (2017). Auger electron spectroscopy. In Microscopy Methods in Nanomaterials Characterization (pp. 363-381). Elsevier.
22. Ilyin, A. M., Guseinov, N. R., & Tulegenova, M. A. (2022). Conical face-field electrostatic energy analyzers for investigating nanomaterials. Journal of Electron Spectroscopy and Related Phenomena, 257, 147203.
23. Hourani, W., Gorbenko, V., Barnes, J. P., Guedj, C., Cipro, R., Moeyaert, J., ... & Martinez, E. (2016). 3D Auger quantitative depth profiling of individual nanoscaled III–V heterostructures. Journal of Electron Spectroscopy and Related Phenomena, 213, 1-10.
24. Shard, A. G. (2012). A straightforward method for interpreting XPS data from core–shell nanoparticles. The Journal of Physical Chemistry C, 116(31), 16806-16813.
25. Cant, D. J., Wang, Y. C., Castner, D. G., & Shard, A. G. (2016). A technique for calculation of shell thicknesses for core–shell–shell nanoparticles from XPS data. Surface and Interface Analysis, 48(5), 274-282.
26. Unger, W. E., Wirth, T., & Hodoroaba, V. D. (2020). Auger electron spectroscopy. In Characterization of Nanoparticles (pp. 373-395). Elsevier.
27. Xu, M., Fujita, D., Gao, J., & Hanagata, N. (2010). Auger electron spectroscopy: a rational method for determining thickness of graphene films. Acs Nano, 4(5), 2937-2945.
28. S.N. Raman, D.F. Paul, J.S. Hammond and K.D. Ilyin, A. M., Guseinov, N. R., & Tulegenova, M. A. (2022). Conical face-field electrostatic energy analyzers for investigating nanomaterials. Journal of Electron Spectroscopy and Related Phenomena, 257, 147203.
29. Kalaga, K., Shkrob, I. A., Haasch, R. T., Peebles, C., Bareno, J., & Abraham, D. P. (2017). Auger electrons as probes for composite micro-and nanostructured materials: application to solid electrolyte interphases in graphite and silicon-graphite electrodes. The Journal of Physical Chemistry C, 121(42), 23333-23346.
30. Baer, D. R., Gaspar, D. J., Nachimuthu, P., Techane, S. D., & Castner, D. G. (2010). Application of surface chemical analysis tools for characterization of nanoparticles. Analytical and bioanalytical chemistry, 396, 983-1002.
31. Kaciulis, S., Mezzi, A., Calvani, P., & Trucchi, D. M. (2014). Electron spectroscopy of the main allotropes of carbon. Surface and Interface Analysis, 46(10-11), 966-969.
32. Zha, X., Walker, C. G., & El-Gomati, M. (2014, June). Auger Electron Spectroscopy in high vacuum: Nanocharacterisation in the Scanning Electron Microscope. In Journal of Physics: Conference Series (Vol. 522, No. 1, p. 012027). IOP Publishing.
33. Xu, M., Fujita, D., & Hanagata, N. (2010). Monitoring electron-beam irradiation effects on graphenes by temporal Auger electron spectroscopy. Nanotechnology, 21(26), 265705.
34. Korin, E., Froumin, N., & Cohen, S. (2017). Surface analysis of nanocomplexes by X-ray photoelectron spectroscopy (XPS). ACS Biomaterials Science & Engineering, 3(6), 882-889.
35. Aronova, M. A., & Leapman, R. D. (2013). Elemental mapping by electron energy loss spectroscopy in biology. Nanoimaging: Methods and Protocols, 209-226.
36. Kapp, N., Studer, D., Gehr, P., & Geiser, M. (2007). Electron energy-loss spectroscopy as a tool for elemental analysis in biological specimens. Electron Microscopy: Methods and Protocols, 431-447.
37. Hagberg, A., Rzhepishevska, O., Semenets, A., Cisneros, D. A., & Ramstedt, M. (2020). Surface analysis of bacterial systems using cryo-X-ray photoelectron spectroscopy. Surface and Interface Analysis, 52(12), 792-801.
38. Andronowski, J. M., Mundorff, A. Z., Davis, R. A., & Price, E. W. (2019). Application of X-ray photoelectron spectroscopy to examine surface chemistry of cancellous bone and medullary contents to refine bone sample selection for nuclear DNA analysis. Journal of Analytical Atomic Spectrometry, 34(10), 2074-2082.
39. Aronova, M. A., & Leapman, R. D. (2012). Development of electron energy-loss spectroscopy in the biological sciences. MRS bulletin, 37(1), 53-62.
40. Andrews, D. J., Barabash, S., Edberg, N. J., Gurnett, D. A., Hall, B. E. S., Holmström, M., ... & Witasse, O. (2016). Plasma observations during the Mars atmospheric “plume” event of March–April 2012. Journal of Geophysical Research: Space Physics, 121(4), 3139-3154.
41. Sauvaud, J. A., Larson, D., Aoustin, C., Curtis, D., Médale, J. L., Fedorov, A., ... & Penou, E. (2008). The IMPACT solar wind electron analyzer (SWEA). The STEREO Mission, 227-239.
42. Barabash, S., Lundin, R., Andersson, H., Brinkfeldt, K., Grigoriev, A., Gunell, H., ... & Thocaven, J. J. (2006). The analyzer of space plasmas and energetic atoms (ASPERA-3) for the Mars Express mission. Space Science Reviews, 126, 113-164.
43. Cara, A., Lavraud, B., Fedorov, A., De Keyser, J., DeMarco, R., Marcucci, M. F., ... & Bruno, R. (2017). Electrostatic analyzer design for solar wind proton measurements with high temporal, energy, and angular resolutions. Journal of Geophysical Research: Space Physics, 122(2), 1439-1450.
44. Kazama, Y. (2013). Designing a toroidal top-hat energy

analyzer for low-energy electron measurement. An introduction to space instrumentation, 181-192.
45. Barabash, S., Lundin, R., Andersson, H., Brinkfeldt, K., Grigoriev, A., Gunell, H., ... & Thocaven, J. J. (2006). The analyzer of space plasmas and energetic atoms (ASPERA-3) for the Mars Express mission. Space Science Reviews, 126, 113-164.
46. Victor, A. L., Zurbuchen, T. H., & Gallimore, A. D. (2006). Top hat electrostatic analyzer for far-field electric propulsion plume diagnostics. Review of scientific instruments, 77(1).
47. Clark, G., Allegrini, F., McComas, D. J., & Louarn, P. (2016). Modeling the response of a top hat electrostatic analyzer in an external magnetic field: Experimental validation with the Juno JADE-E sensor. Journal of Geophysical Research: Space Physics, 121(6), 5121-5136.
48. Nicolaou, G., Wicks, R. T., Rae, I. J., & Kataria, D. O. (2020). Evaluating the performance of a plasma analyzer for a space weather monitor mission concept. Space Weather, 18(12), e2020SW002559.
49. Li, C., Wang, Y., Zhang, H., Li, S., Liu, Z., & Zhao, C. (2018). The analyzer constant of top hat electrostatic analyzer: comparison between theory and simulations. Journal of Instrumentation, 13(12), P12027.
50. Nicolaou, G., Haythornthwaite, R. P., & Coates, A. J. (2022). Resolving Space Plasma Species With Electrostatic Analyzers. Frontiers in Astronomy and Space Sciences, 9, 861433.
51. Engelhart, D. P., Plis, E. A., Ferguson, D., Johnston, W. R., Cooper, R., & Hoffmann, R. C. (2019). Space plasma interactions with spacecraft materials. Plasma Science and Technology-Basic Fundamentals and Modern Applications, 225-245.
52. Garrett, H. B., & Whittlesey, A. C. (2012). Guide to mitigating spacecraft charging effects (Vol. 3). John Wiley & Sons.
53. Thomsen, M. F., Henderson, M. G., & Jordanova, V. K. (2013). Statistical properties of the surface-charging environment at geosynchronous orbit. Space Weather, 11(5), 237-244.
54. Farnell, C. C., Farnell, C. C., Farnell, S. C., & Williams, J. D. (2013, October). Electrostatic analyzers with application to electric propulsion testing. In Proceedings of the 33rd International Electric Propulsion Conference (IEPC'13).
55. Zouros, T. J. M., & Benis, E. P. (2005). Optimal energy resolution of a hemispherical analyzer with virtual entry. Applied Physics Letters, 86(9).
56. Tusche, C., Chen, Y. J., Schneider, C. M., & Kirschner, J. (2019). Imaging properties of hemispherical electrostatic energy analyzers for high resolution momentum microscopy. Ultramicroscopy, 206, 112815.
57. Benis, E. P., & Zouros, T. J. M. (2008). The hemispherical deflector analyser revisited: II. Electron-optical properties. Journal of Electron Spectroscopy and Related Phenomena, 163(1-3), 28-39.
58. Louette, P., Delage, A., Roy, D., Thiry, P. A., & Caudano, R. (1990). An interelectrode distance dependent fringing field correction for the hemispherical deflector analyzer. Journal of Electron Spectroscopy and Related Phenomena, 52, 867-874.
59. Dogan, M., Ulu, M., Gennarakis, G. G., & Zouros, T. J. M. (2013). Experimental energy resolution of a paracentric hemispherical deflector analyzer for different entry positions and bias. Review of Scientific Instruments, 84(4).
60. Sise, O., Ulu, M., Dogan, M., Martinez, G., & Zouros, T. J. (2010). Fringing field optimization of hemispherical deflector analyzers using BEM and FDM. Journal of Electron Spectroscopy and Related Phenomena, 177(1), 42-51.
61. Sise, O., Zouros, T. J. M., Ulu, M., & Dogan, M. (2007). Novel and traditional fringing field correction schemes for the hemispherical analyser: comparison of first-order focusing and energy resolution. Measurement Science and Technology, 18(7), 1853.
62. Yavor, M. I., Belov, V. D., & Pomozov, T. V. (2008). Fringing field correction of the second-order angular aberration in sector field electron energy analyzers. Journal of Electron Spectroscopy and Related Phenomena, 168(1-3), 29-33.
63. Louette, P., Delage, A., Roy, D., Thiry, P. A., & Caudano, R. (1990). An interelectrode distance dependent fringing field correction for the hemispherical deflector analyzer. Journal of Electron Spectroscopy and Related Phenomena, 52, 867-874.
64. Cipriani, F., Leblanc, F., Illiano, J. M., & Berthelier, J. J. (2012). A hemispherical retarding field energy analyzer to characterize spatially and angularly extended electron beams. The European Physical Journal-Applied Physics, 60(2), 21002.
65. Liu, H., Chen, Z., Zhuang, G., Chen, Z., & Xiao, C. (2016). A new application of retarding field analyzer for the electron and ion temperature measurement on the J-TEXT tokamak. Review of Scientific Instruments, 87(11).
66. Baird, M., McGee-Sinclair, R., Lemmer, K., & Huang, W. (2021). Time-resolved ion energy measurements using a retarding potential analyzer. Review of Scientific Instruments, 92(7).
67. Hu, J., Rovey, J. L., & Zhao, W. (2017). Retarding field energy analyzer for high energy pulsed electron beam measurements. Review of Scientific Instruments, 88(1).
68. Zhang, X., Elliott, D. B., Maan, A., Boyle, D. P., Kaita, R., & Majeski, R. (2019). Design and calibration of a retarding field energy analyzer for the LTX-β scrape off layer and modeling of electrostatic potential in a collisionless SOL. Nuclear Materials and Energy, 19, 250-254.
69. Hwang, J., Kim, K. I., Ogawa, T., Cho, B., Kim, D. H., & Park, I. Y. (2020). Study and design of a lens-type retarding field energy analyzer without a grid electrode. Ultramicroscopy, 209, 112880.
70. Hwang, J., Kim, K. I., Ogawa, T., Cho, B., Kim, D. H., & Park, I. Y. (2020). Study and design of a lens-type retarding field energy analyzer without a grid electrode. Ultramicroscopy, 209, 112880.
71. Collinson, G. A., Chornay, D. J., Glocer, A., Paschalidis, N.,

& Zesta, E. (2018). A hybrid electrostatic retarding potential analyzer for the measurement of plasmas at extremely high energy resolution. Review of Scientific Instruments, 89(11).
72. Gulbrandsen, N., Miloch, W. J., & Fredriksen, Å. (2013). Interpretation of ion velocity distributions measured with a grounded retarding field energy analyzer (RFEA) in an inductively coupled helicon plasma. Contributions to Plasma Physics, 53(1), 27-32.
73. Ogasawara, K., Allegrini, F., Desai, M. I., Ebert, R. W., Fuselier, S. A., Jahn, J. M., ... & McComas, D. J. (2018). A double-cusp type electrostatic analyzer for high-cadence solar-wind suprathermal ion observations. Review of Scientific Instruments, 89(11).
74. Bedington, R., Kataria, D. O., & Smith, A. (2014). A highly miniaturized electron and ion energy spectrometer prototype for the rapid analysis of space plasmas. Review of Scientific Instruments, 85(2).
75. Morel, X., Berthomier, M., & Berthelier, J. J. (2017). Electrostatic analyzer with a 3-D instantaneous field of view for fast measurements of plasma distribution functions in space. Journal of Geophysical Research: Space Physics, 122(3), 3397-3410.
76. Floss, C. (2018). Auger spectroscopy in planetary science: elemental analysis of presolar silicate grains.
77. Ilyin, A. M., & Ilyina, I. A. (2014). High-resolving electrostatic charged particles energy analyzer with fine tuning for space investigations. Journal of Instrumentation, 9(08), P08005.
78. Ilyin, A. M., & Ilyina, I. A. (2007). New electrostatic energy analyzer for space plasma measurements. Journal of Instrumentation, 2(01), P01002.
79. Ilyin, A. M., & Ilyina, I. A. (2007). An electrostatic face-field energy analyser for space and plasma measurements. Measurement Science and Technology, 18(3), 724.
80. A.M. Ilyin and B.A. Borisov. Second-order focusing of a bounded cylindrical field for a distant source. Meas.Sci. Technol., 2001, V.12, N11, pp.2015-2017.
81. Ilyin, A. M. (2001). Focusing properties of a bounded cylindrical field. Journal of Electron Spectroscopy and Related Phenomena, 120(1-3), 89-91
82. Ilyin, A. M. (2000). About some focusing properties of a cylindrical field. Journal of Electron Spectroscopy and Related Phenomena, 113(1), 1-2.
83. Ilyin, A. M., & Ilyina, I. A. (2005). New electrostatic energy analysers with a bounded cylindrical field. Measurement Science and Technology, 16(9), 1798.
84. Zashkvara, V. V., & Ilin, A. M. (1973). EFFECT OF TECHNOLOGICAL ERRORS ON FOCUSING OF A CYLINDRICAL MIRROR-TYPE ANALYZER. ZHURNAL TEKHNICHESKOI FIZIKI, 43(9), 1843-1852.
85. Yavor, S. Y., & Baranova, L. A. (1990). Optics of conical electrostatic analysing and focusing systems. Nuclear Instruments and Methods in Physics Research Section A: Accelerators, Spectrometers, Detectors and Associated Equipment, 298(1-3), 421-425.
86. L.A.Baranova and S.Ya. Yavor. Radial cone electron-optical systems . Zh. Techn. Fiziki, 1984, 10, 1999 - 2003.
87. Kazama, Y., Wang, B. J., Wang, S. Y., Ho, P. T., Tam, S. W., Chang, T. F., ... & Asamura, K. (2017). Low-energy particle experiments–electron analyzer (LEPe) onboard the Arase spacecraft. Earth, Planets and Space, 69, 1-13.